HT2009-88205

EVAPORATORS FOR HIGH TEMPERATURE LIFT VAPOR COMPRESSION LOOP FOR SPACE APPLICATIONS

Tadej Semenic
Advanced Cooling Technologies, Inc.
Lancaster, Pennsylvania, USA

Xudong Tang
Advanced Cooling Technologies, Inc.
Lancaster, Pennsylvania, USA

ABSTRACT

An Advanced Vapor Compression Loop (AVCL) for high temperature lift for heat rejection to hot lunar surface during lunar daytime was developed. The loop consists of an evaporator, a compressor, a condenser, and an electronic expansion valve. Different types of evaporators were evaluated in this study: a circular tube evaporator, a circular tube evaporator with a twisted tape, a circular tube evaporator with a wick, and a circular tube evaporator with a wick and a twisted tape. The evaporators were tested with two different compressors. The first was a 0.5hp oil-less compressor and the second was a 5.3hp compressor that used oil as lubricant. A heat exchanger (recuperator) was used to subcool the high pressure liquid and to superheat the low pressure vapor. Tests were performed with and without the recuperator. Vapor superheat during the tests was controlled with an electronic expansion valve controller. The working fluid was R134a.

The results show that the heat source-to-working fluid thermal resistance of the circular tube evaporator with the wick and the twisted tape was one-third of that of the circular tube evaporator. The recuperator was able to decrease the vapor quality at the evaporator inlet and increase the vapor superheat at the compressor inlet. The evaporators without wicks were able to operate at a heat flux of 5.7W/cm^2 with the recuperator and vapor superheat set at 5°C. Evaporators with wicks reached dryout at lower heat fluxes when maintaining superheat at 5°C. However, the wicked evaporators reached a heat flux of 7.6W/cm^2 when decreasing superheat below 5°C. A temperature lift of 70°C was achieved with the 5.3hp compressor.

INTRODUCTION

NASA's new vision for Space Exploration includes returning humans to the Moon by 2020 and the eventual human exploration of Mars. The envisioned first step is to explore the lunar surface with Altair Lunar Lander previously known as Lunar Surface Access Module (LSAM).

The objective of the thermal control systems (TCS) of the Altair Lunar Lander is to maintain the cabin and electronics temperatures within acceptable levels anywhere on the lunar surface during the hot lunar daytime. This is challenging because the lunar surface temperature at the equator can range from -173°C to 121°C [1-5].

The most effective heat rejection method is to radiate the heat to space. The temperature difference between the radiator surface and the heat sink needs to be sufficiently large to ensure a compact radiator. The maximum heat sink temperature is known to be about 47°C at the lunar equator during lunar noon [2]. The temperature of the TCS for the lunar surface system is expected to be about 0°C. Consequently, a temperature lift of at least 50°C is required to reject the waste heat from the surface system to the heat sink.

There exist several TCS technologies [6]. The most promising ones are heat pumps [7] that use electrical energy to remove heat from a lower temperature source to a higher temperature radiator. There exist many different types of heat pumps [7-9]. One of the most common types is Rankine or vapor compression heat pump.

A typical Rankine heat pump consists of a compressor, an evaporator, a condenser, and an expansion valve. It involves two isobaric and two adiabatic processes. The cycle could be either a single refrigerant loop or a cascade (two-stage) refrigerant loop. The condenser of the refrigeration loop could either be a radiator or a heat exchanger between the refrigeration loop and the radiator loop.

There exist many different types of evaporators for the Rankine heat pump. Based on hydraulic channel diameter they can be divided into: macro, small, mini, and micro channel evaporators. Micro/mini-channel evaporators have been extensively studied in the past decade due to their compactness, minimum coolant usage, and superior cooling performance [10-15]. Micro/mini-channel evaporators may handle high heat flux

at low evaporator thermal resistance, but require a high pumping power to overcome a high pressure drop through the channels.

A relatively large density difference between the refrigerant vapor and liquid phases through micro-channels may induce flow instability and pressure oscillation. It was also found that the interaction of the two-phase mixture in the evaporator with the upstream compressed vapor in a flow loop can trigger severe pressure oscillations, which can result in a premature critical heat flux [12]. The micro-channel evaporators are also susceptible to a secondary, parallel channel instability caused by interaction between the channels. This instability is in general milder than the aforementioned instabilities, but is quite random in nature.

To avoid the issues related with micro/mini-channel evaporators this work developed an Advanced Vapor Compression Loop (AVCL) with an advanced evaporator for thermal control of Altair Lunar Lander. The uniqueness of the AVCL concept is in the evaporator design that consists of a porous wick structure and a vortex generating twisted tape. The combination of capillary and centrifugal forces is capable of achieving passive and effective separation of the liquid and vapor phases and consequently improving the evaporator heat flux performance, reducing the heat source temperature, and isothermalizing the heat source.

NOMENCLATURE

E	evaporator
h	enthalpy [kJ/kg]
HEX	recuperator (heat exchanger)
HZ	heat zones
Q	heat [W]
R	thermal resistance [°C/W]
T	temperature [°C]
W	work [W]
x	vapor quality

Subscripts

e	evaporator
l	liquid
v	vapor

METHOD

Small-Scale AVCL

A 500W, small-scale AVCL was build and used to test four different evaporator designs (Figure 1). The AVCL consists of an evaporator, a compressor, a condenser and an electronic expansion valve.

Several additional elements were included in the small scale AVCL to assure proper operation of the compressor and to improve the performance of the AVCL. The evaporator and the transport lines were made of thick wall copper tubing. Two saddle shaped aluminum heater blocks with embedded

cartridge heaters were clumped around the evaporator to simulate the heat source.
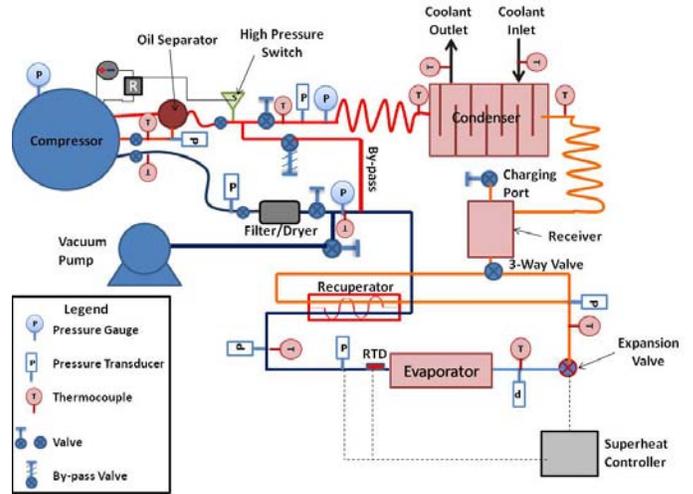
Figure 1: A Small-Scale AVCL

A heat exchanger (recuperator) was used to subcool the liquid refrigerant entering the expansion valve and to superheat the vapor leaving the evaporator. A filter and a drier were used to remove moisture and any solid particles that might be entrained in the vapor.

Two different types of compressors were tested in this work: a 0.5hp Appion G5 Twin piston compressor and a 5.3hp Maneurop MTZ064-3 reciprocating compressor. The Appion compressor is an oil-less compressor, and the Maneurop compressor uses oil as lubricant.

An oil separator was installed at the compressor discharge side to separate the oil from the oil-refrigerant mixture. A high pressure switch after the oil separator was used to turn off the compressor if the discharge pressure would rise above the maximum allowable compressor pressure. A by-pass line with a by-pass valve was used to flow the hot gas to the suction side of the loop during startup and low heat load operations. It had to be assured that at any time during the operation only superheated vapor entered the compressor.

The condenser was a water cooled flat plate heat exchanger (GEA PHE Systems, FP 3x8-14) that used water from a PID-regulated water heater to simulate different heat sink temperatures. An 80-inch (203cm) long vapor coil and a 100-inch (254cm) long liquid coil with diameter 0.245-inch (0.6cm) were used to simulate the distance to between the condenser and the evaporator.

A receiver after the liquid coil was used to store refrigerant while changing the evaporators. After the receiver was located an expansion valve (SEI-0.5 Sporlan electronic expansion valve). The expansion valve together with the compressor controlled the temperature and the mass flow rate of the refrigerant. The valve used an electronically operated stepper motor to precisely control the liquid refrigerant flow. The superheat controller monitored the evaporator outlet

temperature and pressure in real-time, and calculated the thermodynamic states. The controller adjusted the stepper motor and the valve as well as the refrigerant flow rate accordingly to achieve single phase (superheated) vapor at the evaporator outlet.

Figure 1 also shows the locations of the thermocouples (TC) and pressure transducers. Low pressure side used Omega PX603-100G pressure transducers and high pressure side used Omega PX603-1KG pressure transducers. Two TCs and a flow meter were used to measure the temperature and the flow rate of the water flowing into the condenser heat exchanger for the purpose of calorimetry. The temperatures across the evaporator were measured with four equally spaced TCs. The distance between the TCs was 1.4-inch (3.6cm).

The accuracy of the pressure readings was ±0.4PSI (±2.8kPA) on the low pressure side and ±4PSI (±27.6kPa) on the high pressure side. The accuracy of the temperature readings was ±0.1°C.

All the components of the AVCL were well insulated using silicone foam insulation. Thermal conductivity of the insulation was 0.2W/m·K.

Several refrigerants were examined: R-12, R-22, R-125, R-134a, and R143a. R-11 and R-22 were excluded due to environmental concerns. The required flow rates at relevant test conditions for R-125 and R-143a were calculated to be much higher than for the R-134a; therefore, the R-134a was chosen as the working fluid.

Figure 2 shows a simplified model of the AVCL. Two-phase mixture (1) enters the evaporator where the heat applied to the evaporator vaporizes the liquid phase of the mixture. The expansion valve controls the flow through the evaporator so that the vapor at point (2) is superheated for 5°C.
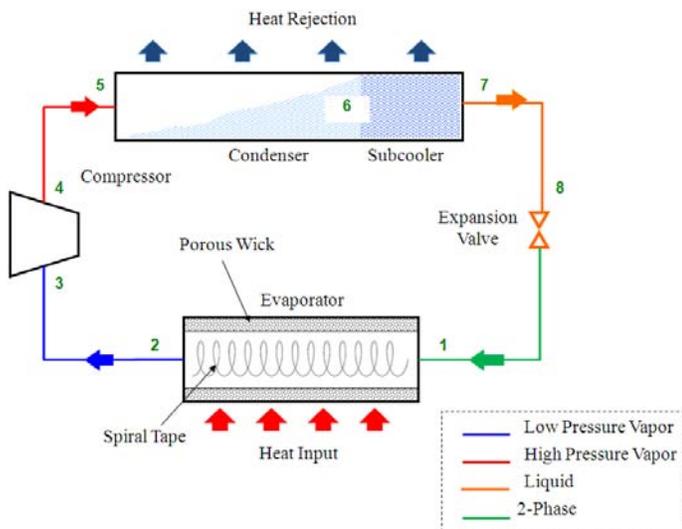
Figure 2: Simplified Model of the AVCL

Superheated vapor at point (3) enters the compressor and gets compressed to a higher pressure and temperature at point (4). The high pressure vapor enters the condenser at point (5)

and is cooled to saturated liquid at point (6) and further subcooled to a lower temperature at point (7). The subcooled liquid flows to the expansion valve inlet (8) and undergoes the reduction in pressure that results in an adiabatic evaporation of a portion of the liquid refrigerant. This lowers the temperature of the fluid (two-phase mixture) to the desired level.

There were four critical positions in the loop: evaporator inlet (1), evaporator outlet (2), condenser inlet (5), and expansion valve inlet (8). As long as the thermodynamics properties of these locations are identified, the operation mechanism and the performance of AVCL is fully defined.

Evaporators
The heat applied to the evaporator outer wall increases the vapor quality of the two-phase mixture entering the evaporator. As the result the flow velocity and momentum increase as the liquid vaporizes. The overall process of heat transfer in a refrigerant evaporator is dominated by two modes. The first mode is nucleate boiling from the heated wall, where the heat transfer coefficient strongly depends on the heat flux. The second mode is forced convection evaporation of the liquid film, where the heat transfer coefficient mainly depends on the mass flow rate and vapor quality. A key to a successful evaporator design is to ensure maximum contact between the liquid phase and the heated wall and minimum vapor interference with the liquid-wall contact.

Our evaporator design includes a phase separator within the evaporator that separates the liquid and vapor phases during the evaporation. The evaporator is made by forming a wick on the inner wall of a circular tube and by press fitting a twisted tape into the tube.

When the two-phase refrigerant mixture enters the evaporator, the twisted tape causes a tangential motion, creating a centrifugal vortex (swirl). The centrifugal force moves the heavier liquid phase toward the tube inner wall to the capillary wick where the heat is applied. The lighter vapor phase largely flows in the center core region. Once the liquid phase contacts the wall it is sucked into the pores of the wick and is evenly distributed to the entire heat input surface. The porous wick also provides extended heat transfer surface for better heat spreading and reduced evaporator thermal resistance.

Five evaporators were made and tested in this study (see Table 1). The evaporators were 7-inches (17.8cm) long circular tubes with diameters 0.75-inches (1.9cm). Total heated evaporator area was 106cm^2.

Table 1: List of the Evaporators Tested

Evaporator	Description	Twisted Tape Pitch (mm)	Wick Thickness (mm)
E1	circular tube	N/A	N/A
E2	circular tube with a twisted tape 1	68	N/A
E3	circular tube with a twisted tape 2	34	N/A
E4	circular tube with a powder wick	N/A	2
E5	circular tube with powder wick and a twisted tape 1	34	2

Evaporator 1 (E1) was made of a smooth circular tube and was used as a baseline. E2 was a circular tube evaporator with a twisted tape (Figure 3). E3 was similar to E2, but had a twisted tape with more turns (smaller pitch). E4 was a circular tube evaporator with a wick and E5 was a circular tube evaporator with both a wick and a twisted tape.
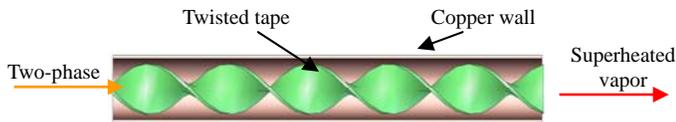
Figure 3: Evaporator E2 Design

Test Procedure

Initially, the AVCL was evacuated and the R134a refrigerant was charged into the receiver. It was calculated based on the condenser, the receiver, and the line volume that 3lb (1.4kg) of the refrigerant is required. After starting the compressor several heat loads were applied to the evaporator. Evaporators E1, E2, E4, and E5 were tested with Appion compressor at 200W and all five evaporators were tested with the Maneurop compressor from 400-600W (3.8-5.7W/cm^2). Steady state was assumed when temperatures did not change for more than 1°C in 15minutes. Steady temperatures and pressures were used to calculate evaporator thermal resistances and thermodynamic states at different locations of the loop. All evaporators were tested with and without a recuperator. A three-way valve after the receiver was used to direct the flow either to the recuperator or directly to the expansion valve.

RESULTS AND DISCUSSIONS

After recording temperatures and pressures at different steady power loads, the evaporator surface temperature, T_e, was calculated as the average temperature of the four evaporator temperature readings (shown as *HZ1* to *HZ4* in Figure 4). Vapor temperature, T_v, was calculated as the average temperature between the vapor inlet and the vapor outlet temperature. Evaporator thermal resistance was calculated as:

$$R_{ev} = \frac{(T_e - T_v)}{Q_{in}} \qquad (1)$$

Where Q_{in} is the power supplied to the heater calculated as the product of the voltage and the current. Heat losses from the heater were neglected since the heater temperature during the tests was below or close to the ambient temperature.

Figure 4 shows temperatures and pressures for evaporator E2 tested with the recuperator. We can see that the evaporator temperatures started running away when the heat load was increased from 600W to 700W. Maximum heat load for this evaporator, Q_{max}, was 600W.

(a)

(b)
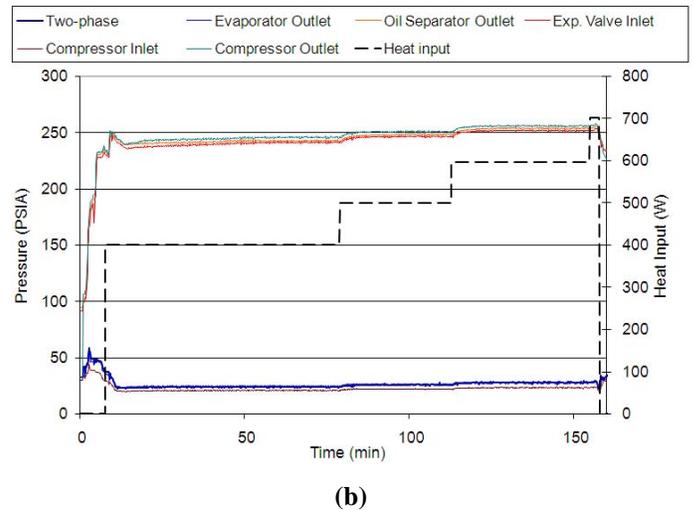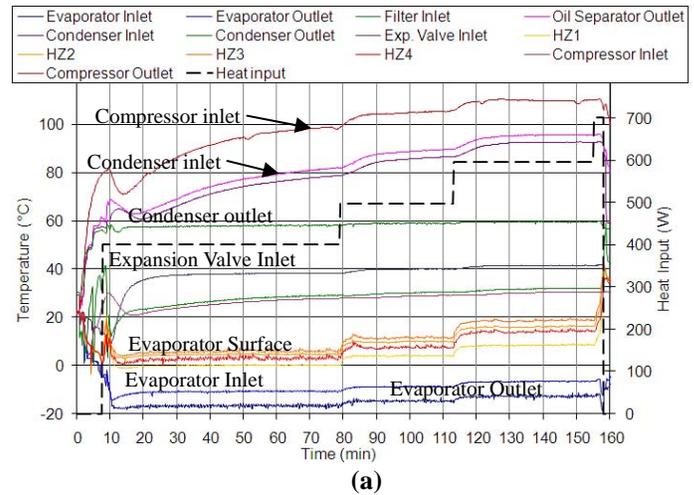
Figure 4: (a) Temperatures and (b) Pressures for Evaporator E2 Tested with a Recuperator

During the test, the expansion valve maintained a constant vapor superheat of 6°C between the evaporator inlet and the evaporator outlet. When changing the heat load from one power level to another, the evaporator temperatures did not experience transient temperature spikes. As the power increased, the difference between the maximum and the

minimum evaporator (heat zone) temperature increased from 5.8°C at 400W to 10.1°C at 600W.

Liquid temperature at the expansion valve inlet increased from 38°C to 41°C while condensing temperature increased from 60°C to 62°C when changing the power from 400-600W. This means that the condenser and the recuperator subcooled the liquid for 21°C.

The pressure chart (Figure 4 b) shows that the highest pressure in the loop was at the compressor outlet (point (4) in Figure 2) and that the pressure decreased around the loop to the lowest pressure at the compressor inlet (point (3) in Figure 2). Average pressure drop on the high pressure side was 4PSI or 27.6kPa (within the accuracy of the measurement) and the average pressure drop on the low pressure side was 3.5PSI (24.1kPa). The majority of the pressure drop was through the filter/drier and the oil separator.

Table 2 summarizes test results for the four evaporators tested with Appion compressor. Evaporating temperature (temperature of the two-phase mixture) was found to be in average 3°C lower when using a recuperator.

Since both, temperature and pressure were measured upstream and downstream of the expansion valve, the vapor quality at the evaporator inlet was obtained as,

$$x = \frac{(h_{e,inlet} - h_l)}{(h_v - h_l)} \tag{2}$$

Where, $h_{e,inlet}$ is the enthalpy of the two-phase mixture at the evaporator inlet, h_l liquid enthalpy at saturation temperature of the two-phase mixture and h_v vapor enthalpy at saturation temperature of the two-phase mixture. All enthalpies were obtained from NIST [16]. Since the expansion valve was well insulated, it was assumed that the expansion through the expansion valve was an isenthalpic (constant enthalpy) process.

Table 2: Evaporator Performances Using Appion Compressor

No	HEX*	Q_{in}	T_e	T_v	R_{ev}	x
		W	°C	°C	°C /W	%
E1	NO	200	20.4	10.5	**0.050**	18.1%
	YES	200	15.0	5.5	**0.047**	18.3%
E2	NO	200	12.8	6.2	**0.033**	17.3%
	YES	200	11.9	5.5	**0.032**	12.7%
E3	NO	200	10.8	5.8	**0.025**	18.2%
	YES	200	8.0	4.5	**0.017**	13.9%
E5	NO	200	8.1	5.1	**0.015**	18.4%
	YES	200	6.9	4.2	**0.014**	13.2%

* *HEX-recuperator (heat exchanger)*

When using a recuperator, the vapor quality got reduced in average for 4%. By comparing thermal resistances of different types of the evaporators, we can see that the thermal resistance of the evaporator E5 was one third of that of the baseline evaporator E1.

All five evaporators were tested with the Maneurop compressor. The results of the tests are summarized in Table 3.

Table 3: Evaporator Performances Using Maneurop Compressor

No	HEX	$Q_{in,max}$	Q_{in}	T_e	T_v	R_{ev}*	x
		W	W	°C	°C	°C /W	%
E1	NO	500	506	16.6	-8.3	**0.050**	47%
	YES	600	501	11.8	-11.6	**0.047**	35%
E2	NO	500	505	10.2	-10.2	**0.041**	48%
	YES	600	499	8.4	-11.5	**0.040**	36%
E3	NO	500	502	11.6	-9.3	**0.042**	48%
	YES	600	500	12.6	-11.1	**0.047**	36%
E4	NO	Temperature runaway at <400W					
	YES	400	398	-3.8	-11.1	**0.018**	34%
E5	NO	400	400	-2.4	-9.8	**0.019**	47%
	YES	500	496	-0.9	-9.5	**0.017**	34%

* *Thermal resistance was calculated at the heat load Q*

We can see that E1, E2, and E3 reached Q_{max} at 600W when using a recuperator and at 500W when not using the recuperator. Also subcooling the liquid with the recuperator reduced the vapor quality in average for 13%. It is believed that at lower vapor quality, more liquid phase is in contact with a heated wall resulting in higher Q_{max}. Evaporating temperature was in average 2°C lower when using a recuperator. Similar to the tests with Appion compressor, the thermal resistance of the evaporator E5 is still one third of the thermal resistance of the baseline evaporator E1. This indicates that the wick and the twisted tape improved the liquid distribution in the evaporator and resulted in lower evaporator thermal resistance.

It is known that the oil separator is not 100% efficient by separating oil from the refrigerant and a small amount of the oil is expected to enter the evaporator wick. The oil did not seem to have a detrimental effect on the performance of the evaporators with the wicks.

Interestingly, the evaporators with the wick (E4 and E5) reached Q_{max} at lower heat load than other evaporators. The reason for this was found to be the expansion valve controller that keeps opening and closing the expansion valve in a way to maintain superheated vapor at the evaporator outlet. When the expansion valve controller reads the superheat that is lower than the preset superheat, it starts closing the valve. This results that the wick starts to starve the liquid and consequently it starts to dry out. It is very difficult for a dry wick to rewet unless the heat load to the wick is reduced. It is also possible that the time between two consecutive valve openings is too short for the wick to rewet.

To verify this hypothesis, the position of the expansion valve was set constant depending on the heat load and a two-phase mixture was allowed to exit the evaporator. Evaporator E5 was used for this test. Table 4 shows that by increasing the refrigerant flow rate and reducing the vapor quality at the

evaporator inlet, the evaporator thermal resistance can be further reduced. Furthermore, the Q_{max} was increased from 500W to 800W. We can see that if the wick has sufficient amount of the liquid, the evaporator thermal resistance can be reduced and the maximum heat load increased.

Table 4: Tests for E5 with Recuperator at Lower Vapor Superheat

Superh eat	Q_{max}	T_e	T_v	R_{ev}	x	ΔT_{lift}
°C	W	°C	°C	°C /W	%	°C
4.2	496	-0.9	-9.5	**0.017**	34%	71.5
3.3	498	-1.3	-10.0	**0.017**	34%	71.2
0	595	-1.7	-5.9	**0.007**	19%	67
0	717	1.2	-3.8	**0.007**	23%	65.6
0	803	5.3	0.7	**0.006**	21%	65.5

The last column in Table 4 shows a temperature lift, ΔT_{lift}, defined as the difference between the condensing and the evaporating temperature. Figure 5 shows a temperature lift for evaporator E5 tested with the recuperator and two different compressors.
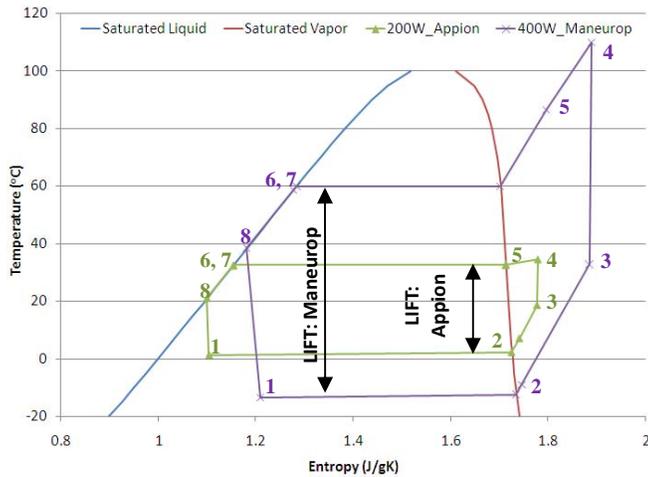
Figure 5: Temperature Lift for E5 Tested with a Recuperator and two Different Compressors

The temperature lift for 200W with Appion compressor was 30°C while the temperature lift for 400W with Maneurop compressor was 71°C. The temperature lift for Maneurop compressor could be further increased if increasing the sink temperature.

The coefficient of performance, COP, was defined as

$$COP = \frac{Q_{in}}{W_{compressor}} \qquad (3)$$

where Q_{in} is the power applied to the evaporator and $W_{compressor,}$ the electrical work consumed by the compressor. Since the Maneurop compressor was purchased for the full-scale AVCL

with the heat load above 3kW, the COP for tests presented in this work was only 0.1 to 0.2. COP for Maneurop MTZ064-3 compressor at -10°C evaporating temperature and 60°C condensing temperature is 1.32 [17]. A heat load at these conditions is 4.2kW. COP for the tests with the Appion compressor was 0.5-0.6.

The future work will focus on improving the expansion valve superheat control and the reduction of vapor quality at the evaporator inlet. Additionally, the COP will be increased by testing the evaporators close to the compressor optimum performance point.

CONCLUDING REMARKS

A small-scale Advanced Vapor Compression Loop (AVCL) was build and used to test four different types of evaporators: a circular tube evaporator, a circular tube evaporator with a twisted tape, a circular tube evaporator with a wick, and a circular tube evaporator with a wick and a twisted tape. The evaporators were tested with two different compressors and with or without a recuperator.

The evaporator with a wick and a twisted tape was able to remove heat at one third of the thermal resistance of the circular tube evaporator. Performance degradation of the wicked evaporators due to presence of compressor lubricant in the loop was not observed. It was found that the evaporators without wick reached higher maximum heat flux than the evaporators with the wick. The reason for this was found to be the expansion valve superheat control that forced the wick to become partially dry. The hypothesis was partially confirmed by keeping the expansion valve at a constant setting to allow a two-phase mixture to exit the evaporator. The results showed that the critical heat flux got increased from 5.6 to 7.6W/cm^2 and the thermal resistance got reduced from 0.017°C/W to 0.006°C/W when increasing the refrigerant flow and keeping the wick saturated.

When using a 0.5hp compressor and 200W heat load a temperature lift of 30°C was achieved and when using a 5.3hp compressor and 400W heat load a temperature lift of 71°C was achieved. The compressors were not optimized for the small-scale AVCL tests resulting in a coefficient of performance (COP) of only 0.1-0.6. The future work will address the control of vapor quality and the increase of the COP by running a compressor at the optimal operating point.

REFERENCES

[1] Swanson T., Radermacher R., Costello F., Moore J., and Mengers D., 1990, "Low-temperature thermal control for a lunar base", *20th Intersociety Conference on Environmental Systems*, July 9-12, 1990, Williamburg, Virginia.

[2] Ewert, M., 1993, "Investigation of lunar base thermal control system options", *23th International Conference on Environmental Systems*, July 12~15, 1993, Colorado Springs, Colorado.

[3] Nikanpour D. and De-Parolis L., 1996, "Space-based heat pumps for a lunar lander/rover thermal control", *26th International Conference on Environmental Systems*, July 8-11, 1996, Montery, California.

[4] Aidoun Z., Nikanpour D. and De-Parolis L., 1996, "Vapor compression heat pump for a lunar lander/rover thermal control", *26th International Conference on Environmental Systems*, July 8-11, 1996, Monterey, California.

[5] Morton, R.D., Bergeron, D., Hurlbert, K.M., Ewert, M. and Cornwell, J., 1998, "Proof of Concept high lift heat pump for a lunar base" *SAE Paper No. 9816.*

[6] Simonson, M.J., DeBarro, J.T., 1988, "Conceptual design of a lunar base thermal control system," *Symposium on Lunar Bases and Space Activities in the 21st Century,* Houston, TX, April 1988.

[7] Sridhar, K.R., and Gorrmann, M., 1996, "Thermal Control System for Lunar Base Cooling,"*Journal of Thermophysics and Heat Transfer,* **10** (3), pp. 490-496.

[8] Hanford, A.J., and Ewert, M.K., 1996, "Advanced Active Thermal Control Systems Architecture Study," *NASA TM-104822.*

[9] Lambert, M.A., and Jones, B.J., 2007, "Comparison of Heat Pumps for Permanet Lunar Base, *Journal of Thermophysics and Heat Transfer,* **21** (1), pp. 209-218.

[10] Agostini, B., Watel, B., Bontemps, A., and Thonon, B., 2003, "Boiling Heat Transfer in Mini-Channels: Influence of the Hydraulic Diameter," *Proc. 21st IIR International Congress of Refrigeration.*

[11] Agostini, B., Bontemps, A., 2005, "Vertical Flow Boiling of Refrigerant R134a in Small Channels," *International Journal of Heat and Fluid Flow,* **26,** pp.296-306.

[12] Qu, W., Mudawar, I., 2003, "Measurement and prediction of pressure drop in two-phase micro-channel heat sinks, *Int. J. Heat Mass Transfer* **46,** pp. 2737–2753.

[13] Lee, J., Mudawar, I., 2005, "Two-phase flow in high-heat flux micro-channel heat sink for refrigeration cooling applications: Part I - Pressure drop characteristics," *Int. J. Heat Mass Transfer*, **48**, pp. 928-940.

[14] Lee, J., Mudawar, I., 2005,"Two-phase flow in high-heat-flux micro-channel heat sink for refrigeration cooling applications: Part II - Heat transfer characteristics, *Int. J. Heat Mass Transfer*, **48**, pp. 941-955.

[15] Lee, J., Mudawar, I., 2008, "Fluid flow and heat transfer characteristics of low temperature two-phase micro-channel heat sinks - Part 1: Experimental methods and flow visualization results, *Int. J. Heat Mass Transfer* **51,** pp.4315-4326.

[16] Thermophysical properties of fluids, *NIST*, http://webbook.nist.gov/chemistry/fluid/

[17] Maneurop Reciprocating Compressors, *Technical Data Sheet*, http://doc.3c-e.com/danfoss/odsg/pdf/FRCC-UD-090430-022415.pdf